

# Hypervelocity Impact Fusion with Compressed Deuterium-Tritium Targets

Silviu Olariu

Institute of Physics and Nuclear Engineering

Department of Fundamental Experimental Physics

P.O. Box MG-6, 76900 Magurele, Bucharest, Romania

## Abstract

The neutron yields observed in inertial confinement fusion experiments for higher convergence ratios are about two orders of magnitude smaller than the neutron yields predicted by one-dimensional models, the discrepancy being attributed to the development of instabilities. We consider the possibility that ignition and a moderate gain could be achieved with existing laser facilities if the laser driver energy is used to produce only the radial compression of the fuel capsule to high densities but relatively low temperatures, while the ignition of the fusion reactions in the compressed fuel capsule will be effected by a synchronized hypervelocity impact. A positively-charged incident projectile can be accelerated to velocities of  $3.5 \times 10^6$  m s<sup>-1</sup>, resulting in ignition temperatures of about 4 keV, by a conventional low- $\beta$  linac having a length of 13 km if deuterium-tritium densities of 570 g cm<sup>-3</sup> could be obtained by laser-driven compression.

## 1 Introduction

The standard approach to inertial confinement fusion is based on the deposition in the outer layers of a deuterium-tritium fuel capsule of sufficient energy to produce a hot central spot of moderate density but high temperature, while the remaining fuel mass has a high density but a relatively low temperature [1]. Deuterium-tritium fuel densities of 20 to 40 g cm<sup>-3</sup> have been reported in cryogenic target experiments conducted at the University of Rochester [2], and compressed core densities estimated to be 120 g cm<sup>-3</sup> have been reported in tests conducted at the Osaka

University [3]. High deuterium-tritium densities have also been obtained at Lawrence Livermore National Laboratory and at the Centre d'Etudes de Limeil-Valenton. There is a consensus that ignition and a moderate gain for inertial confinement fusion can be achieved with a driver energy of the order of 1 MJ, subject to stringent uniformity requirements.

While target gains of the order of 100 are predicted by one-dimensional simulations for a MJ laser input [4], the neutron yields observed in inertial confinement fusion experiments for higher convergence ratios are about two orders of magnitude smaller than the neutron yields calculated with one-dimensional models, the discrepancy being attributed to non-uniformities of the drive flux and to the development of instabilities [5]. The present goal of inertial confinement fusion research is to achieve ignition and a moderate gain  $G > 1$  [6].

In the conventional approach to inertial confinement fusion, both the high-density fuel mass and the hot central spot are supposed to be produced by the deposition of the driver energy in the outer layers of the fuel capsule. While high densities can be produced indeed, this approach appears to be less efficient in igniting the fusion processes, as mentioned previously. It is proposed in this paper that the driver energy should be used only to produce the radial compression of the fuel capsule to high densities but relatively low temperatures, while the ignition of fusion reactions in the compressed fuel capsules should be effected by a synchronized hypervelocity impact. The hypervelocity-impact ignition of fusion reactions in a compressed fuel capsule is expected to result in higher gains than those actually possible with the conventional approach, for the same driver energy.

In Sec. 2 we describe the general processes involved in the hypervelocity-impact ignition of nuclear fusion reactions in laser-compressed fuel pellets. In Sec. 3 we discuss the amount of electric charge which can be carried by an incident projectile and then determine an expression for the length of the linac that would accelerate the projectile to the required velocity. A case study is reported in Sec. 4, where an acceleration length of 13 km is obtained on the assumption that deuterium-tritium densities of  $570 \text{ g cm}^{-3}$  could be obtained by laser-driven compression. The impact-heating rates are estimated in this case to be as high as  $1.1 \times 10^{19} \text{ W cm}^{-2}$ . At pressures of about  $10^{-11}$  torr in the accelerating column the heating and the ionization produced by the interaction of the incident projectile with the background gas molecules is found to be within acceptable limits. In Sec. 5 we mention the possibility to build a hypervelocity accelerator and a linear electron-positron collider as parallel structures on the same site, thus sharing the costs of the cryogenic units, vacuum technique and of the tunnel. An alternative approach is based on the generation of an electric-field wave front with the aid of successively activated switches.

## 2 Hypervelocity-impact ignition of laser-compressed fuel pellets

We shall consider an incident projectile consisting of a spherical shell of radius  $r$  and thickness  $\delta$ , made of a material having a high mechanical tensile strength and a high evaporation field. This projectile we suppose to be incident with a velocity of  $3.5 \times 10^6 \text{ m s}^{-1}$  upon a large-yield fuel target at rest. The collision of the incident projectile and of the large-yield target takes place inside a double cylindrical high-Z case, as shown in Fig. 1. A laser pulse is converted at the walls of the larger cavity into X rays, which compress the incident projectile and the large-yield target in high-density states. The difference in the compression times of the incident projectile and of the fuel target is compensated by the fact that the X-ray pressure is exerted on the incident projectile only for the final part of its path. A second, short laser pulse is projected inside the smaller cavity to ensure the uniform illumination of the incident projectile during the entrance into the larger cavity. The main laser pulse and the movement of the incident projectile are synchronized such that the collision should take place when the densities are the highest. The collision converts the kinetic energy of the incident projectile into thermal energy, the resulting temperature being supposed sufficient to ignite the fusion reactions between the deuterium-tritium nuclei contained by the fuel target at rest. The fusion reactions thus ignited will be propagated in the entire volume of the large-yield target.

The possibility to use hypervelocity impact to ignite nuclear fusion reactions has been previously investigated especially with regard to the type of the linear acceleration that would provide kinetic energies of the order of 1 MJ to projectiles with a mass of about 0.1 g [7]-[11]. A numerical one-dimensional study of deuterium-tritium ignition in impact-fusion targets found necessary shell energies of about 30 MJ [12]. The magnitude of the large threshold energy in impact fusion in the absence of laser compression can be explained by the asymmetry of the pressures exerted during the collision of two macroscopic bodies.

Thus, by decoupling the mechanism producing the compression of the fuel from the mechanism producing the heating of the fuel, it becomes possible to use the spherically-symmetric pressure exerted by a radiation driver to compress the fuel to a high-density state, and at the same time to use the high energy-transfer rates characteristic to impact processes to efficiently heat the compressed fuel, with the aid of a comparatively small amount of kinetic energy.

We shall assume that the velocities required for the ignition of nuclear fusion reactions are obtained by accelerating the positively-charged projectiles along a series of coaxial tubular electrodes

connected alternatively to two bus bars and supplied by a radio-frequency power source. This arrangement, due to Wideroe [13], is used when the ratio of the velocity of the charged projectile to the velocity of light is small compared to 1. The acceleration of macroparticles based on an electrostatic charge carried by the projectile has been previously regarded as uncompetitive because of the length of the accelerator [8],[11],[14], but those estimates have been based on the presumption of a MJ kinetic energy for a 0.1 g projectile incident with a velocity of about  $1.5 \times 10^5 \text{ m s}^{-1}$ . However, if the fuel target at rest is driven in the high-density state before the collision, the kinetic energy threshold is substantially lowered. Moreover, since the required incident velocity of about  $3.5 \times 10^6 \text{ m s}^{-1}$ , which would result in an ignition temperature of about 4 keV, is one order of magnitude larger than the velocity used in the afore-mentioned evaluations, then the mass of the incident projectile becomes very small, of the order of  $10^{-6} \text{ g}$ , and for masses of this magnitude the efficient acceleration approach is that based on the electrostatic charge.

### 3 Acceleration of the incident projectile

We assume that the incident projectile is a hollow sphere of radius  $r$  and thickness  $\delta$ , of aspect ratio

$$A = r/\delta, \tag{1}$$

This moving hollow sphere is compressed inside the case shown in Fig. 1 to a full sphere of radius  $r_0$ , so that the material of the projectile undergoes a compression by a factor

$$P = 3r^2\delta/r_0^3, \tag{2}$$

At the moment of the impact, the density of the compressed deuterium-tritium fuel of the target at rest is  $n_0$ , the fuel being initially compressed by a factor

$$F = n_0/n_s, \tag{3}$$

where  $n_s = 4.5 \times 10^{22} \text{ cm}^{-3}$  is the regular solid-state density of equimolar deuterium-tritium. We shall express the various quantities in this paper in terms of the dimensionless parameters  $A, P, F$ .

We assume moreover that the kinetic energy of the compressed projectile of radius  $r_0$  is converted with a certain efficiency  $\eta_{tot}$  into thermal energy at temperature  $T_0$  of the compressed deuterium-tritium fuel over a sphere of the same radius  $r_0$ , situated in the impact region. According to Brueckner and Jorna [15], ignition of the compressed deuterium-tritium fuel will take place if

$$r_0 = r_c/F, \tag{4}$$

where  $r_c = 2.81 \times 10^{-2}$  m when  $kT_0 = 4$  keV, and the initial thermal energy  $E_{th}$  to produce ignition of the deuterium-tritium sphere of radius  $r_0$  is ,

$$E_{th} = E_u/F^2, \quad (5)$$

where  $E_u = 7.99 \times 10^9$  J for the same initial temperature of  $kT_0 = 4$  keV. Then from Eqs. (1)-(5), the initial radius of the projectile is

$$r = \frac{r_c}{F} \left( \frac{AP}{3} \right)^{1/3}, \quad (6)$$

and the thickness of the spherical shell is

$$\delta = \frac{r_c}{F} \left( \frac{P}{3A^2} \right)^{1/3}. \quad (7)$$

We shall now determine the amount of electric charge  $q_\delta$  which can be carried by the incident projectile. The variables which limit the amount of positive electric charge which can be carried by a hollow sphere are the mechanical strength, which opposes the electrostatic repulsion forces, and the surface electric field, which determines the field-evaporation and the field-ionization phenomena. It can be shown that the maximum electric field  $E_\delta$  which can be mechanically sustained by a spherical shell made of a material of tensile strength  $\sigma$ , of radius  $r$  and thickness  $\delta \ll r$ , is given by

$$E_\delta = (4\delta\sigma/\epsilon_0 r)^{1/2}, \quad (8)$$

in SI units. The ideal tensile strength of a material can be estimated as [16]

$$\sigma = E/10, \quad (9)$$

where  $E$  is the Young's modulus. At the same time, the electric field at the surface of the projectile must not exceed the field-evaporation limit. Large surface electric fields are encountered in field-ion microscopy [17],[18], where observations are frequently made at fields comparable to the field-evaporation limit, of the order of  $5 \times 10^{10}$  V m<sup>-1</sup>. For spherical shells, the more stringent condition is that ensuring the mechanical stability of the charged shell, Eq. (8). Then the maximum amount of positive electric charge which can be carried by the fuel capsule is

$$q_\delta = 4\pi\epsilon_0 r^2 E_\delta, \quad (10)$$

which can be written with the aid of Eqs. (6)-(8) as

$$q_\delta = \frac{8\pi}{3^{2/3}} \epsilon_0^{1/2} \sigma^{1/2} A^{1/6} P^{2/3} \frac{r_c^2}{F^2}. \quad (11)$$

We shall consider that the total efficiency  $\eta_{tot}$  with which the kinetic energy of the incident projectile is transformed into thermal energy of the compressed deuterium-tritium fuel is a product of three factors. The first of these factors, which can be obtained from the conservation of the energy and momentum during the impact, is  $(1 + m_\delta/m_0)^{-1}$ , where

$$m_\delta = 4\pi r^2 \delta \rho_Z \quad (12)$$

is the mass of the incident projectile of density  $\rho_Z$ , and

$$m_0 = \frac{4\pi r_0^3}{3} m_{DT} n_0 \quad (13)$$

is the initial mass of deuterium-tritium fuel whose temperature is raised to  $kT_0$  as a result of the impact,  $m_{DT} = 4.17 \times 10^{-27}$  kg being the average of the masses of a deuterium nucleus and of a tritium nucleus. The second factor takes into account the fact that the thermal energy is distributed between the deuterium-tritium nuclei, the nuclei of the material of the projectile and the corresponding electrons, and is given by

$$\left(1 + \frac{3}{2}(Z+1) \frac{r^2 \delta n_Z}{r_0^3 n_0}\right)^{-1}$$

where the number  $Z$  characterizes the material of the projectile. The third factor is an empirical efficiency  $\eta$ , by which we take into account the deviations from the assumptions of our model.

Then the total efficiency is of the form

$$\eta_{tot} = \eta \left(1 + \frac{P \rho_Z}{F \rho_s}\right)^{-1} \left(1 + \frac{1}{2}(Z+1) \frac{P n_Z}{F n_s}\right)^{-1}, \quad (14)$$

where  $\rho_s = m_{DT} n_s$  is the density of solid deuterium-tritium,  $\rho_s = 0.19$  g cm<sup>-3</sup>.

The potential difference  $\Phi_\delta$  accelerating the incident projectile of charge  $q_\delta$  to an energy which, converted with efficiency  $\eta_{tot}$ , results in a thermal energy  $E_{th}$  at a temperature  $kT_0 = 4$  keV of the compressed deuterium-tritium fuel is

$$\Phi_\delta = \frac{E_{th}}{\eta_{tot} q_\delta}, \quad (15)$$

and can be expressed in terms of the dimensionless parameters  $A, P, F$  as

$$\Phi_\delta = \frac{3^{2/3}}{8\pi\eta} \left(1 + \frac{P \rho_Z}{F \rho_s}\right) \left(1 + \frac{1}{2}(Z+1) \frac{P n_Z}{F n_s}\right) \frac{E_u A^{-1/6} P^{-2/3}}{\epsilon_0^{1/2} \sigma^{1/2} r_c^2}, \quad (16)$$

As mentioned previously, we suppose that the positively-charged projectiles are accelerated to the required energy by the electric field extant in the gaps between a series of tubular electrodes connected to a radio-frequency source. Since the low- $\beta$  values result in relatively low applied

frequencies, the electric field extant in a gap of length  $d$  between successive electrodes can be estimated as the static breakdown field for the same electrodes [19],

$$E = Kd^{-1/2}. \quad (17)$$

The average accelerating field  $E_{av}$  is reduced by a factor  $2^{3/2}/\pi$  with respect to  $E$  because of the sinusoidal time dependence, and moreover it is reduced by a factor of  $1/2$  when we take into account the length of the drift tubes, supposed equal to the gap length,

$$E_{av} = (2^{1/2}/\pi)Kd^{-1/2}. \quad (18)$$

where the value  $K = 2.4 \times 10^6$ , in SI units, corresponds to copper electrodes with an area of a few square centimeters. We shall determine the radius  $a$  of the tubular electrodes from the requirement that the electric field of the charged projectile at the distance  $a$  from its center should not exceed the breakdown field, Eq. (17), for the distance  $a$ ,

$$a = (q_\delta/4\pi\epsilon_0 K)^{2/3}. \quad (19)$$

and shall consider that the gap spacing  $d$  is a certain multiple  $N$  of the diameter  $2a$  of the tube,

$$d = 2Na \quad (20)$$

The average electric field can then be written in terms of  $A, P, F$  as

$$E_{av} = \frac{3^{2/9} K^{4/3} \epsilon_0^{1/6} F^{2/3}}{2^{1/3} \pi N^{1/2} \sigma^{1/6} r_c^{2/3} A^{1/18} P^{2/9}}, \quad (21)$$

so that the length of the accelerator  $L_\delta = \Phi_\delta/E_{av}$  is

$$L_\delta = \frac{3^{4/9} N^{1/2}}{2^{8/3} \eta} \left(1 + \frac{P}{F} \frac{\rho_Z}{\rho_s}\right) \left(1 + \frac{1}{2}(Z+1) \frac{P}{F} \frac{n_Z}{n_s}\right) \frac{E_u A^{-1/9} P^{-4/9} F^{-2/3}}{\epsilon_0^{2/3} \sigma^{1/3} r_c^{4/3} K^{4/3}}, \quad (22)$$

The radius of the drift tubes is

$$a = \frac{2^{2/3} \sigma^{1/3} r_c^{4/3} A^{1/9} P^{4/9}}{3^{4/9} \epsilon_0^{1/3} K^{2/3} F^{4/3}}, \quad (23)$$

and the electric field of the projectile at distance  $a$  is

$$E(a) = \frac{3^{2/9}}{2^{5/6} N^{1/2}} \frac{\epsilon_0^{1/6} K^{4/3} F^{2/3}}{\sigma^{1/6} r_c^{2/3} A^{1/18} P^{2/9}} \quad (24)$$

The electric field at the surface of the incident projectile,  $E_s = q_\delta/4\pi\epsilon_0 r^2$ , is

$$E_s = 2\epsilon_0^{-1/2} \sigma^{1/2} A^{-1/2}. \quad (25)$$

The mass of the incident projectile, previously written in Eq. (12), is

$$m_\delta = \frac{4\pi}{3} \frac{r_c^3}{F^3} P \rho_Z. \quad (26)$$

The final energy of the incident projectile is

$$E_\delta = E_{th}/\eta_{tot}, \quad (27)$$

and the final velocity  $v$  of the projectile, calculated from the relation  $m_\delta v^2/2 = E_\delta$ , is

$$v = \frac{3^{1/2}}{2^{1/2}\pi^{1/2}\eta^{1/2}} \left(1 + \frac{P}{F} \frac{\rho_Z}{\rho_s}\right)^{1/2} \left(1 + \frac{1}{2}(Z+1) \frac{P}{F} \frac{n_Z}{n_s}\right)^{1/2} \frac{E_u^{1/2} F^{1/2} P^{-1/2}}{\rho_Z^{1/2} r_c^{3/2} \eta^{1/2}}. \quad (28)$$

The average force acting on the projectile, calculated as  $F_\delta = q_\delta E_{av}$ , is

$$F_\delta = \frac{2^{8/3}}{3^{4/9} N^{1/2}} \epsilon_0^{2/3} \sigma^{1/3} r_c^{4/3} K^{4/3} \frac{A^{1/9} P^{4/9}}{F^{4/3}}, \quad (29)$$

and the average acceleration of the projectile is

$$a_\delta = \frac{2^{2/3} 3^{5/9} \epsilon_0^{2/3} \sigma^{1/3} K^{4/3} A^{1/9} F^{5/3}}{\pi N^{1/2} r_c^{5/3} P^{5/9} \rho_Z} \quad (30)$$

The time of transit of the projectile through the accelerator, calculated as  $t_\delta = (2L_\delta/a_\delta)^{1/2}$ , is

$$t_\delta = \frac{\pi^{1/2} N^{1/2}}{2^{7/6} 3^{1/18} \eta^{1/2}} \left(1 + \frac{P}{F} \frac{\rho_Z}{\rho_s}\right)^{1/2} \left(1 + \frac{1}{2}(Z+1) \frac{P}{F} \frac{n_Z}{n_s}\right)^{1/2} \frac{E_u^{1/2} r_c^{1/6} P^{1/18} \rho_Z^{1/2}}{\epsilon_0^{2/3} \sigma^{1/3} K^{4/3} A^{1/9} F^{7/6}}, \quad (31)$$

Finally the specific charge of the projectile is

$$\frac{q_\delta}{m_\delta} = \frac{24^{1/3} \epsilon_0^{1/2} \sigma^{1/2} A^{1/6} F}{r_c P^{1/3} \rho_Z}. \quad (32)$$

## 4 Case study

If we examine the expressions of the acceleration length  $L_\delta$ , Eq. (22), and of the potential difference  $\Phi_\delta$ , Eq. (16), we see that small values of the density  $\rho_Z$  and large values of the tensile strength  $\sigma$  of the material of the projectile result in low values of  $L_\delta$  and  $\Phi_\delta$ . We shall consider that the material of the projectile is beryllium, with  $Z = 4$ ,  $\rho_Z = 1.85 \text{ g cm}^{-3}$  and an ideal tensile strength, Eq. (9),  $\sigma = 2.96 \times 10^{10} \text{ N m}^{-2}$ . The values of the acceleration length  $L_\delta$  and of the potential difference  $\Phi_\delta$  have been represented in Fig. 2 and respectively Fig. 3 as functions of the ratio  $P/F$ , for  $F=1000$  and  $F=3000$ , taking the aspect ratio, Eq. (1),  $A=10$ , the empiric efficiency introduced in Eq. (14)  $\eta=0.5$  and the parameter  $N$  defined in Eq. (20)  $N=2$ . The length  $L_\delta$  is minimized in the case of a beryllium projectile when  $P/F = 0.0348$ , and the potential  $\Phi_\delta$  is minimized when  $P/F = 0.0611$ , while  $F$  is as large as possible.

We shall discuss two cases, one when the parameters  $P, F$  defined in Eqs. (2),(3) are  $P = 20, F = 1000$ , and a second case when  $P = 60, F = 3000$ , the other parameters being  $A = 10, \eta = 0.5, N = 2$ . We kept the compression factor  $P$  of the material of the moving projectile as small as



possible, so that  $P/F = 0.02$ , resulting in values of  $L_\delta$  and  $\Phi_\delta$  slightly greater than the minimum values. We assume that the compressed deuterium-tritium fuel is impact-heated to a temperature  $kT_0 = 4$  keV, so that  $r_c = 2.81 \times 10^{-2}$  m,  $E_u = 7.99 \times 10^9$  J, as mentioned previously in Eqs. (4),(5).

In the case when  $P = 20$  and  $F = 1000$ , the radius of the projectile is  $r = 114$   $\mu\text{m}$  and the thickness of the spherical shell is  $\delta = 11$   $\mu\text{m}$ . The density of the beryllium projectile is increased before the impact by a factor  $P = 20$ , to  $37$   $\text{g cm}^{-3}$ . The radius of the compressed fuel region, of initial density  $n_0 = 190$   $\text{g cm}^{-3}$ , and which is heated by impact to a temperature  $kT_0 = 4$  keV, is  $r_0 = 28$   $\mu\text{m}$ , and the initial thermal energy of the deuterium-tritium fuel is  $E_{th} = 7990$  J. The kinetic energy of the projectile is converted into thermal energy of the compressed deuterium-tritium fuel with a total efficiency  $\eta_{tot} = 0.36$ . The charge carried by the projectile is  $q_\delta = 5.28 \times 10^{-8}$  C, the accelerating potential is  $\Phi_\delta = 410$  GeV, and the average accelerating field is  $E_{av} = 9.27 \times 10^6$  V  $\text{m}^{-1}$ . The electric field at the surface of the beryllium projectile is  $E_s = 3.65 \times 10^{10}$  V  $\text{m}^{-1}$ , compared to the desorption field of beryllium of  $5.36 \times 10^{10}$  V  $\text{m}^{-1}$  [20]. The mass of the incident projectile is  $m_\delta = 3.43 \times 10^{-9}$  kg, the final velocity of the projectile is  $v = 3.55 \times 10^6$  m  $\text{s}^{-1}$ , and the final energy of the projectile is  $E_\delta = 2.16 \times 10^4$  J. The radius of a drift tube is  $a = 3.39$  mm, the distance between the tubes is  $d = 1.35$  cm, and the electric field of the projectile at distance  $a$  is  $E(a) = 2.06 \times 10^7$  V  $\text{m}^{-1}$ . The length  $L$  of the accelerator is  $L_\delta = 44.3$  km. The average force on the projectile is  $F_\delta = 0.49$  N, the average acceleration of the projectile is  $a_\delta = 1.42 \times 10^8$  m  $\text{s}^{-2}$ , and the time of transit of the projectile through the accelerator is  $t_\delta = 25$  ms. The specific charge of the projectile is  $q_\delta/m_\delta = 15.3$  C  $\text{kg}^{-1}$ . The frequency of the accelerating field, calculated as  $f = v/4d$ , increases from 184 kHz at the low-velocity end, for an initial velocity of the projectile of  $10^4$  m  $\text{s}^{-1}$ , to 65 MHz at the high-velocity end. For 90 % of the accelerator length, the frequency will be, however, greater than 20 MHz.

In the case when  $P = 60$ ,  $F = 3000$ , the radius of the projectile is  $r = 54$   $\mu\text{m}$  and the thickness of the spherical shell is  $\delta = 5.4$   $\mu\text{m}$ . The density of the beryllium projectile is increased before impact by a factor  $P = 60$ , to  $111$   $\text{g cm}^{-3}$ . The radius of the compressed fuel region, of initial density  $n_0 = 570$   $\text{g cm}^{-3}$ , and which is heated by impact to a temperature  $kT_0 = 4$  keV, is  $r_0 = 9.3$   $\mu\text{m}$ , and the initial thermal energy of the deuterium-tritium fuel is  $E_{th} = 887$  J. The kinetic energy of the projectile is converted into thermal energy of the compressed deuterium-tritium fuel with a total efficiency  $\eta_{tot} = 0.36$ , the same as in the previous case because  $\eta_{tot}$  depends only on the ratio  $P/F$ . The charge carried by the projectile is  $q_\delta = 1.22 \times 10^{-8}$  C, the accelerating potential is  $\Phi_\delta = 197$  GeV, and the average accelerating field is  $E_{av} = 1.51 \times 10^7$  V  $\text{m}^{-1}$ . The electric

field at the surface of the beryllium projectile is  $E_s = 3.65 \times 10^{10} \text{ V m}^{-1}$ , the same as in the previous case. The mass of the incident projectile is  $m_\delta = 3.82 \times 10^{-10} \text{ kg}$ , the final velocity of the projectile is  $v = 3.55 \times 10^6 \text{ m s}^{-1}$ , the same as previously, and the final energy of the projectile is  $E_\delta = 2409 \text{ J}$ . The radius of a drift tube is  $a = 1.28 \text{ mm}$ , the distance between the tubes is  $d = 5.1 \text{ mm}$ , and the electric field of the projectile at distance  $a$  is  $E(a) = 3.35 \times 10^7 \text{ V m}^{-1}$ . The length of the accelerator is  $L_\delta = 13.0 \text{ km}$ . The average force on the projectile is  $F_\delta = 0.18 \text{ N}$ , the average acceleration of the projectile is  $a_\delta = 4.82 \times 10^8 \text{ m s}^{-2}$ , and the time of transit of the projectile through the accelerator is  $t_\delta = 7.3 \text{ ms}$ . The specific charge of the projectile is  $q_\delta/m_\delta = 31.9 \text{ C kg}^{-1}$ . The frequency of the accelerating field, calculated as  $f = v/4d$ , increases from 489 kHz at the low-velocity end, for an initial velocity of the projectile of  $10^4 \text{ m s}^{-1}$ , to 173 MHz at the high-velocity end. For 90 % of the accelerator length the frequency will be, however, greater than 54 MHz.

In order that the collision of the incident projectile and of the fuel target should take place when the densities have their highest values it is necessary that

$$v\tau = D - r_0 - R_c, \quad (33)$$

where  $\tau$  is the time required for the compression of the incident projectile,  $D$  is the distance from the projectile entrance into the large cavity to the center of the target at rest, as shown in Fig. 1,  $r_0, R_c$  are respectively the compressed radii of the incident projectile and of the target at rest, and  $v$  is the velocity of the projectile given by Eq. (28). Since the time required for the compression of the relatively small capsule is of the order of  $\tau = 1 \text{ ns}$ , the product  $v\tau$  is of the order of  $v\tau = 3.5 \text{ mm}$ . If the lifetime  $\tau_c$  of the compressed state of the projectile is of the order of  $\tau_c = 0.1 \text{ ns}$ , the position of the projectile before collision must be defined with an accuracy of less than about  $v\tau_c = 0.35 \text{ mm}$ . The time required for the compression of the large-yield target can be expected to be of the order of 10 ns, which means that the main driver pulse is applied when the distance between the projectile and the target is of about 3.5 cm. The duration of the secondary laser pulse, applied in the small cavity when the projectile enters into the large cavity, can be estimated as  $4r/v$ , which is 128 ps for the 114  $\mu\text{m}$  projectile and 61 ps for the 54  $\mu\text{m}$  projectile. This is only an order-of-magnitude estimate, and further detailed analysis is required to determine whether the moment of the impact can actually be synchronized with the moments when the incident projectile and the fuel target are in the high-density states.

The impact-heating of the fuel, produced during the collision of the compressed incident projectile with the compressed target at rest, takes place in a time estimated as  $2r_0/v_0$ , where  $v_0 = (3kT_0/m_{DT})^{1/2}$  is the thermal velocity of the fuel nuclei at the temperature  $kT_0 = 4 \text{ keV}$ ,

$v_0 = 6.78 \times 10^5 \text{ m s}^{-1}$ . The impact-heating time of the fuel sphere of radius  $r$  is then 82.8 ps for the 114  $\mu\text{m}$  projectile, and 27.6 ps for the 54  $\mu\text{m}$  projectile. In order to estimate the energy-transfer rates, we can consider that the conversion of the incident kinetic energy into heat is effected over the cross-sectional area  $\pi r_0^2$  of the compressed incident projectile. Then the impact-heating rate for the 114  $\mu\text{m}$  projectile, obtained by dividing the 7990 J of thermal energy to the 82.8 ps impact-heating time and the area  $2.48 \times 10^{-5} \text{ cm}^2$ , would be  $3.88 \times 10^{18} \text{ W cm}^{-2}$ , and the impact-heating rate for the 54  $\mu\text{m}$  capsule, obtained by dividing the 887 J of thermal energy to the 27.6 ps impact-heating time and the cross-sectional area  $2.75 \times 10^{-6} \text{ cm}^2$ , would be  $1.16 \times 10^{19} \text{ W cm}^{-2}$ . The very high values of the energy-transfer rates show that the hypervelocity impact is appropriate indeed for the ignition of the fusion processes, but we emphasize that these impact-heating rates are possible only in conjunction with the laser precompression of the fuel.

The fusion processes ignited in the region of impact will be propagated in the entire volume of the large-yield target at rest. Since the burning front advances supersonically, the hydrodynamic expansion associated with the eccentric position of the ignition region appears to be of secondary importance. The hypervelocity-impact ignition of large-yield fuel targets does not require additional accelerating length, because the ignition criterion, Eq. (5), involves the compression  $F = n_0/n_s$ , and does not depend on the total energy yield.

In the system of reference of the projectile, there is an oscillatory electric field which produces an alternating electric polarization of the projectile. In order to estimate the heating produced by the electric currents associated with the motion of electricity in the beryllium shell, we shall regard the metallic shell as a series  $RC$  circuit, the resistance  $R$  being of the order of  $R = \rho_{Be}/6\delta$  and the capacitance of the order of  $C = \pi\epsilon_0 r$ , where  $\rho_{Be}$  is the resistivity of beryllium. The amplitude of the oscillatory potential difference is of the order of  $E_{av}r$  and the frequency of the order of  $\omega = \pi v/d$ . Then the power dissipated in the beryllium shell is of the order of  $\pi^4 \epsilon_0^2 \rho_{Be} r^4 v^2 E_{av}^2 / 12 \delta d^2$ . For a room-temperature electrical resistivity of beryllium  $\rho_{Be} = 4.0 \times 10^{-8} \Omega \text{ m}$ , and a room-temperature specific heat of beryllium of  $1.8 \text{ J g}^{-1} \text{ K}^{-1}$ , the temperature increase of the beryllium shell during the acceleration will be of about  $8.9 \times 10^{-6} \text{ K}$  for the 114  $\mu\text{m}$  projectile and  $4.9 \times 10^{-5} \text{ K}$  for the 54  $\mu\text{m}$  projectile. The small temperature increase is due to the small dimensions of the projectile.

A more important source of heating is the friction with the molecules of the low-pressure gas extant in the acceleration column. If we consider that each gas molecule contributes a thermal energy  $mv^2/2$  by colliding with the projectile, the energy transferred to the beryllium shell over an acceleration length  $L_\delta$  will be  $(mv^2/2)\pi r^2 L_\delta n$ , where  $m$  is the mass of a gas molecule and  $n$  is the concentration of these molecules. If we assume that the background air pressure is  $10^{-11} \text{ torr}$ ,

the temperature increase of the beryllium shell will be 31 K for the 114  $\mu\text{m}$  projectile, and 19 K for the 54  $\mu\text{m}$  projectile.

We can estimate the charge collected by the projectile via the collisions with the background air molecules as  $eZ_{air}\pi r^2 L_\delta n$ . For a residual pressure of  $10^{-11}$  torr, and for  $Z_{air} = 14.4$ , the charge collected by the 114  $\mu\text{m}$  projectile is  $1.47 \times 10^{-9}$  C compared to the total charge  $q_\delta = 5.28 \times 10^{-8}$  C, and the charge collected by the 54  $\mu\text{m}$  projectile is  $1.00 \times 10^{-10}$  C compared to the total charge  $q_\delta = 1.22 \times 10^{-8}$  C.

We mention that the electrostatic energy  $q_\delta^2/4\pi\epsilon_0 r_0$  of the projectile of charge  $q_\delta$ , compressed to a sphere of radius  $r_0$ , is 0.89 J for the 114  $\mu\text{m}$  projectile, and 0.14 J for the 54  $\mu\text{m}$  projectile. Thus, the fact that the projectile is charged does not significantly alter the process of compression from radius  $r$  to radius  $r_0$ .

## 5 Accelerator choices

The radio-frequency power required to activate a 44 km or a 13 km accelerator can be reduced to acceptable values by operating at superconducting temperatures. Although very different in scope and realization, we mention at this point that several projects of linear electron-positron colliders at energies in the 500 GeV region are presently under consideration, the active length being 6.6 km for the CERN's Linear Collider CLIC, and 20 km for the TeV Superconducting Linear Accelerator TESLA [21]. If extended to 2 TeV, the length of the CLIC accelerator would be  $2 \times 16$  km [22]. One possibility would be to build a hypervelocity accelerator and a linear electron-positron collider as parallel structures on the same site, thus sharing the costs of the cryogenic units, vacuum technique and of the tunnel. The case of a linear electron-positron collider would be strengthened if parts of the hardware could be used for an applied research project like the hypervelocity-impact ignition of fusion processes.

If we assume that 10 incident projectiles would be accelerated per second for energy production, the accelerating structure is amenable to pulsed and modular excitation, improving the energy efficiency of the accelerator, so that a charged projectile would actually be under the action of a radio-frequency wave front.

The fact that a single macroscopic particle is accelerated at a time in a hypervelocity accelerator renders possible an alternative design which avoids the use of radio-frequency power altogether. In this design, the accelerating line consists of a series of coaxial tubular electrodes and one bus bar held at a static high positive potential, of the order of  $10^5$  V, the accelerated projectile moving

along the common axis of the tubes. Each drift tube is connected to the high-voltage bar via a gas-insulated, three-electrode spark gap having the structure shown schematically in Fig. 4. The upper electrode T is connected to the drift tube, the lower electrode A is connected to the high-voltage bar, and the electrode F is lying in the proximity of T and has initially the same potential as T, for example a zero potential. When the positively-charged projectile is inside the drift tube, the electrode T becomes polarized positively with respect to F, and that initiates a spark across the close gap between T and F. The ionization thus created then initiates the main discharge between T and A, at the end of which the potential of the electrode T and of the drift tube to which it is connected becomes highly positive. The electric field between the drift tube thus activated and the next tube accelerates the projectile toward the latter tube, which is then activated when the projectile passes through it, and this process of positive charging of the drift tubes is continued all along the path of the projectile. After the acceleration of the projectile is completed, the drift tubes are discharged, the potential of the bus bar restored to its initial high positive value, and another projectile can then be accelerated along the line.

We mention that a 10 m long linac of this type would accelerate the  $114 \mu\text{m}$  projectile considered in Sec. 4 to a velocity of  $53 \text{ km s}^{-1}$ , and the  $54 \mu\text{m}$  projectile to a velocity of  $98 \text{ km s}^{-1}$ .

Another possibility is to excite the accelerating structure by highvoltage pulses of a few picosecond duration, produced by photodiode switches triggered from laser pulses [23].

The costs of current linac projects are estimated at about 1 M\$ per GeV [24], and it is possible that less stringent beam requirements should significantly reduce these costs. While the single-particle linear accelerator envisaged in this work is very different from the afore-mentioned colliders, this comparison suggests however that the cost of a 500 GeV hypervelocity accelerator for impact-fusion research might represent a relatively small fraction of the cost of a reference project like the International Thermonuclear Experimental Reactor tokamak, estimated at  $10^{10}$  \$.

## 6 Conclusions

In this work we have considered the possibility of using the hypervelocity impact of laser-compressed pellets as an ignition mechanism of nuclear fusion processes. The acceleration of an incident projectile to velocities of about  $3.5 \times 10^6 \text{ m s}^{-1}$ , which would result in an ignition temperature of about 4 keV of the compressed deuterium-tritium fuel, can be achieved by positively charging the projectile to the limits permitted by the mechanical rigidity and by the evaporation fields. The accelerating fields can be produced either by a low- $\beta$  linac operating at superconducting temperatures, or by

an electric-field wavefront generated with the aid of sparkgap switches successively activated by the moving charged capsule. An accelerator length of 13 km was estimated on the assumption that deuterium-tritium densities of  $570 \text{ g cm}^{-3}$  could be obtained by laser-driven compression.

The purpose of this paper was of introducing the concept of hypervelocity ignition of fusion reactions in laser-compressed fuel targets. The analysis of this work suggests that existing laser facilities used for inertial confinement fusion research may have the capability to achieve ignition and a moderate gain when used in conjunction with hypervelocity acceleration. At the same time, the development of MJ driver energy remains a necessity for the compression of large-yield targets. Detailed further work is needed however to assess the physical efficiency of the impact ignition mechanism, and to determine the parameters of the accelerating structure and the associated costs.

## References

- [1] J. Nuckolls, L. Wood, A. Thiessen and G. Zimmerman, *Nature* 239 (1972) 139.
- [2] R. L. McCrory et al., *Nature* 335 (1988) 225; F. J. Marshall et al., *Phys. Rev. A* 40 (1989) 2547.
- [3] S. Nakai et al., in *Plasma Physics and Controlled Nuclear Fusion Research, 14<sup>th</sup> Conference Proceedings, Wurzburg 1992, vol. 3 (IAEA Vienna, 1993)*, p. 13.
- [4] K. Mima et al., ref. 3, p. 381.
- [5] M. Andre et al, ref. 3, p. 23; H. Takabe et al., ref. 3, p. 143; T. Yamanaka, ref. 3, p. 151.
- [6] M. M. Sluyter, ref. 3, p. 3.
- [7] F. Winterberg, *Atomkernenergie Kerntechnik* 33 (1979) 302; 36 (1980) 60; 43 (1983) 104; *Phys. Fluids B* 4 (1992) 3350.
- [8] J. N. Brittingham, *Atomkernenergie Kerntechnik* 36 (1980) 130.
- [9] R. L. Garwin, R. A. Muller and B. Richter, *Atomkernenergie Kerntechnik* 35 (1980) 300.
- [10] K. Wendell Chen, *Atomkernenergie Kerntechnik* 36 (1980) 50.
- [11] R. S. Hawke, *Atomkernenergie Kerntechnik* 38 (1981) 35.
- [12] R. M. Zubrin and F. L. Ribe, *IEEE Trans. Plasma Sci.* 17 (1989) 459.

- [13] M. Stanley Livingston and J. P. Blewett, Particle Accelerators (McGrawHill, New York, 1962), p. 312.
- [14] F. Winterberg, Atomkernenergie Kerntechnik 37 (1981) 200.
- [15] K. A. Brueckner and S. Jorna, Rev. Mod. Phys. 46 (1974) 325.
- [16] A. H. Cottrell, The Mechanical Properties of Matter (Wiley, New York, 1964), p. 235.
- [17] E. W. Muller, Field Ionization and Field Ion Microscopy, in Adv. Electronics and Electron Physics vol. XIII, edited by L. Marton (Academic Press, New York, 1960), p. 83.
- [18] K. M. Bowkett and D. A. Smith, FieldIon Microscopy (North Holland, Amsterdam, 1970).
- [19] R. Hawley and A. A. Zaky, Conduction and Breakdown in High Vacuum, in Progress in Dielectrics vol. 7, edited by J. B. Birks (Heywood, London, 1967), p. 115.
- [20] Ref. 17, p. 102.
- [21] R. Settles and G. Coignet, CERN Courier, November 1992, p. 23.
- [22] W. Wunsch, CERN Courier, September 1993, p. 1.
- [23] B. W. Montague, Europhys., News, January 1987, p. 4.
- [24] B. Richter, Europhys. News, October 1991, p. 184.

## Figure captions

Fig. 1. Ignition of fusion reactions by the hypervelocity impact of an incident projectile of velocity  $v$  with a large-yield fuel target at rest. The collision takes place inside the larger cavity of a double cylindrical high- $Z$  case, which converts a laser pulse into X-rays which then drive the incident projectile and the large-yield target at rest into high-density states. The difference in the compression times of the incident capsule and of the large-yield target is compensated by the fact that the X-ray pressure is exerted on the incident projectile only for the final part of its path. A second, short laser pulse is projected inside the smaller cavity to ensure the uniform illumination of the incident projectile during its entrance into the larger cavity.  $D$  is the distance from the incident projectile entrance into the large cavity to the center of the fuel target at rest.

Fig. 2. Accelerator length  $L_\delta$  as a function of the ratio  $P/F$ , for the values  $F = 1000$  and  $F = 3000$ . It is assumed that the material of the projectile is beryllium, and  $A = 10, \eta = 0.5, N = 2$ .

Fig. 3. Potential difference  $\Phi_\delta$  as a function of the ratio  $P/F$ , for the values  $F = 1000$  and  $F = 3000$ . It is assumed that the material of the projectile is beryllium, and  $A = 10, \eta = 0.5, N = 2$ .

Fig. 4. Gas-insulated, three-electrode spark gap connecting a drift tube to a positive high-voltage bar. The upper electrode T is connected to the drift tube, the lower electrode A is connected to the high-voltage bar, and F is lying in the proximity of T and has initially the same potential as T. When the positively-charged capsule is inside the drift tube, the electrode T becomes positively charged with respect to F, and that initiates a spark across the close gap between T and F. The ionization thus created then initiates the main discharge between T and A, at the end of which the potential of the electrode T and of the drift tube to which it is connected becomes highly positive.



Fig. 1

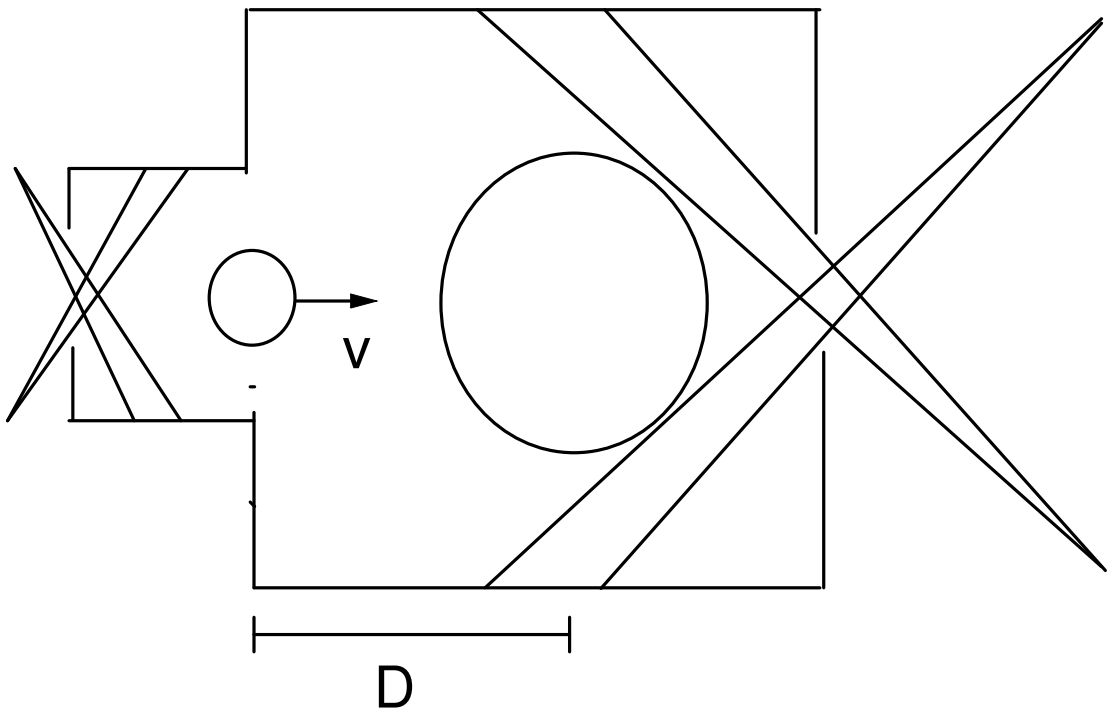




Fig. 2

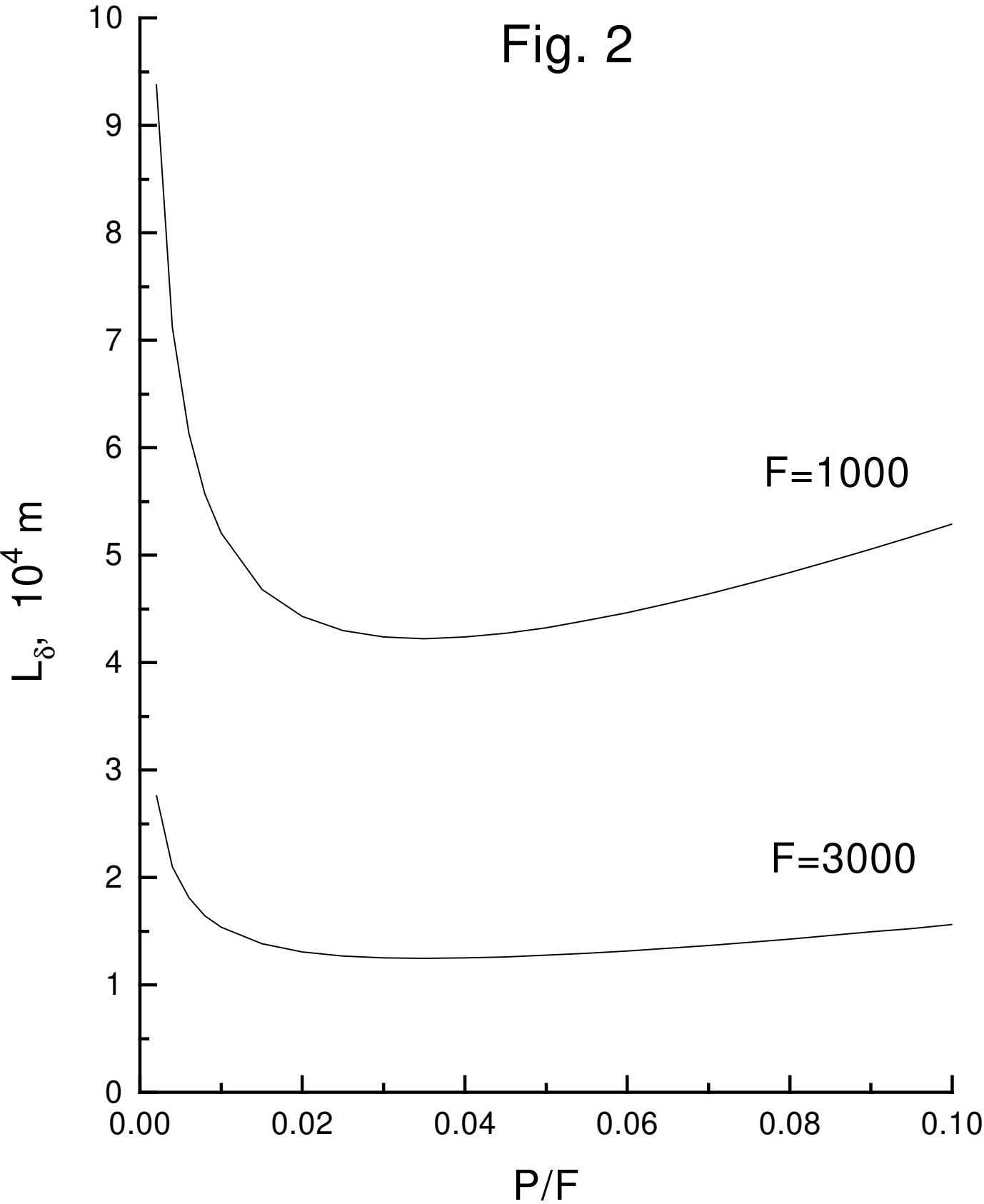




Fig. 3

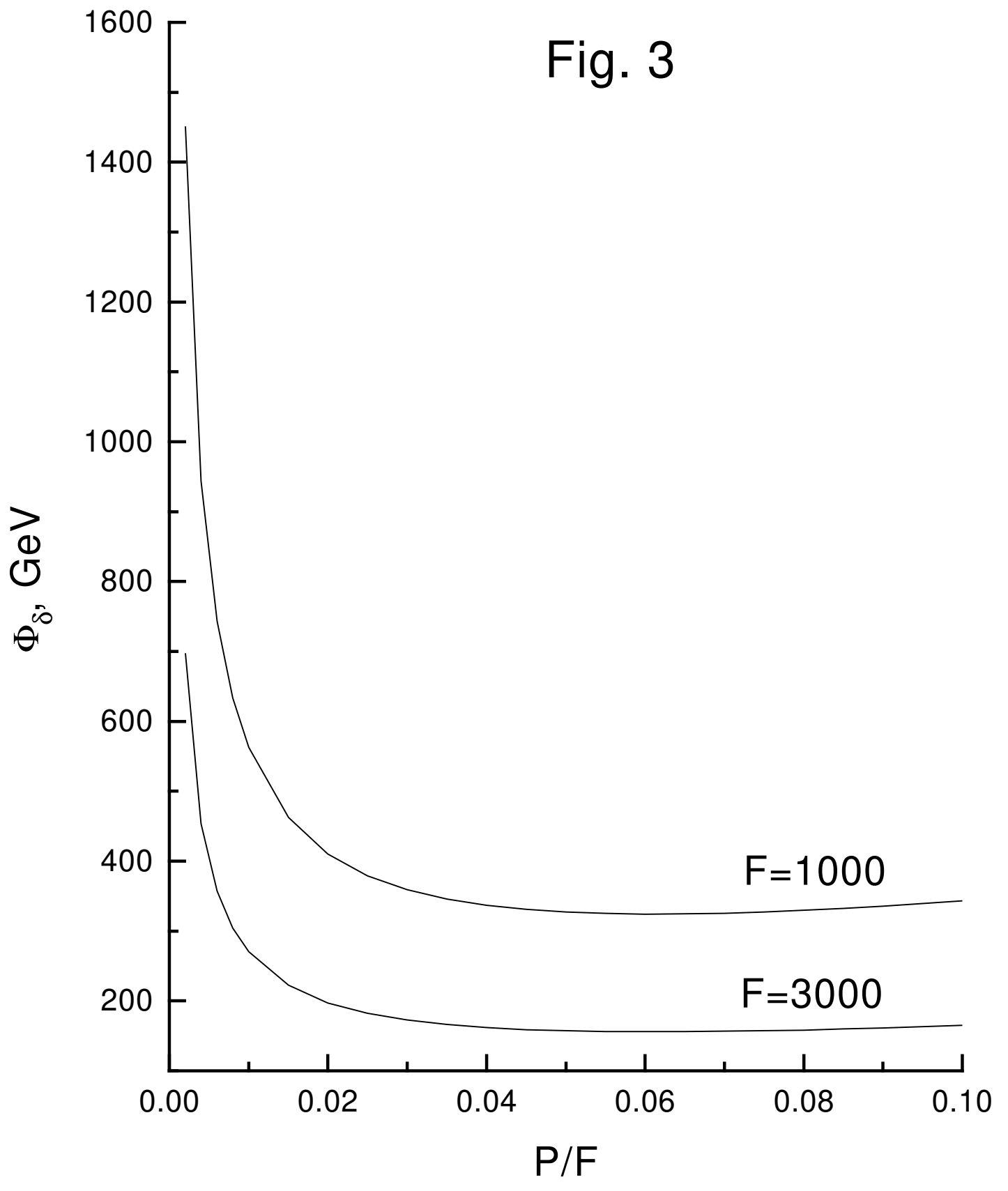




Fig. 4

